THE JOURNAL OF BIOLOGICAL CHEMISTRY VOL. 286, NO. 37, pp. 32300–32312, September 16, 2011


# Hepatic Nuclear Factor 1α (HNF1α) Dysfunction Down-regulates X-box-binding Protein 1 (XBP1) and Sensitizes β-Cells to Endoplasmic Reticulum Stress*[S]

Received for publication, April 5, 2011, and in revised form, July 14, 2011 Published, JBC Papers in Press, July 22, 2011, DOI 10.1074/jbc.M111.247866

**Clare L. Kirkpatrick[‡], Andreas Wiederkehr[§], Mathurin Baquié[‡], Dmitry Akhmedov[‡], Haiyan Wang[¶¶], Benoit R. Gauthier[¶], Ildem Akerman[‖**‡‡], Hisamitsu Ishihara[§§], Jorge Ferrer[‖**‡‡], and Claes B. Wollheim[‡1]**

*From the [‡]Department of Cell Physiology and Metabolism, Centre Médical Universitaire, Université de Genève, 1 Rue Michel-Servet, 1211 Genève 4, Switzerland, the [§]Nestlé Institute of Health Sciences, 1015 Lausanne, Switzerland, the [¶]Andalusian Center for Molecular Biology and Regenerative Medicine, Avda. Américo Vespucio, Parque Científico y Tecnológico Cartuja 93, Sevilla 41092, Spain, the [‖]Genomic Programming of Beta Cells Laboratory, Institut d'Investigacions Biomèdiques August Pi i Sunyer, 08036 Barcelona, Spain, **Endocrinology, Hospital Clínic de Barcelona, 08036 Barcelona, Spain, [‡‡]CIBER de Diabetes y Enfermedades Metabólicas Asociadas, 08036 Barcelona, Spain, the [§§]Division of Diabetes and Metabolic Medicine, Nihon University School of Medicine, Tokyo 173-8610, Japan, and [¶¶]F. Hoffmann-La Roche AG, PRBD-Metabolic Diseases, CH-4070 Basel, Switzerland*

**Correct endoplasmic reticulum (ER) function is critical for the health of secretory cells, such as the pancreatic β-cell, and ER stress is often a contributory factor to β-cell death in type 2 diabetes. We have used an insulin-secreting cell line with inducible expression of dominant negative (DN) HNF1α, a transcription factor vital for correct β-cell development and function, to show that HNF1α is required for *Xbp1* transcription and maintenance of the normal ER stress response. DN HNF1α expression sensitizes the β-cell to ER stress by directly down-regulating *Xbp1* transcription, whereas *Atf6* is unaffected. Furthermore, DN HNF1α alters calcium homeostasis, resulting in elevated cytoplasmic calcium and increased store-operated calcium entry, whereas mitochondrial calcium uptake is normal. Loss of function of XBP1 is toxic to the β-cell and decreases production of the ER chaperone BiP, even in the absence of ER stress. DN HNF1α-induced sensitivity to cyclopiazonic acid can be partially rescued with the chemical chaperone tauroursodeoxycholate. Rat insulin 2 promoter-DN HNF1α mouse islets express lower levels of *BiP* mRNA, synthesize less insulin, and are sensitized to ER stress relative to matched control mouse islets, suggesting that this mechanism is also operating *in vivo*.**

Maturity onset diabetes of the young 3 (MODY3)[2] is caused by heterozygous mutations in the transcription factor *Hnf1α* (1), which lead to a primary defect in β-cell function without insulin resistance. Almost 200 MODY3 mutations in *Hnf1α* have been characterized, with missense mutations occurring most frequently, whereas the appearance of frameshift or nonsense mutations is also observed. MODY3 mutations often act through haploinsufficiency (2), but they can also act through a dominant negative mechanism, as is the case for the (frequently occurring) frameshift mutation P291 fsinsC (3, 4). HNF1α was originally discovered as a regulator of hepatic gene expression but has since been found to be expressed in the pancreas (5) and involved in transcription of β-cell-specific genes (6, 7). However, genome-wide studies have also demonstrated that its effects on gene expression in the liver and pancreatic islet are strikingly different (8). To characterize the role of HNF1α in β-cells, a dominant negative (DN) mutant has been used, which carries a substitution of 83 amino acids in its DNA-binding domain, whereas its dimerization domain remains intact (Fig. 1*A*). This artificial DN mutant forms non-functional dimers with the endogenous protein, preventing it from activating its target genes (9). This has led to the discovery that in insulin-secreting INS-1 cells, suppression of HNF1α activity following induction of the DN gene impairs metabolism-secretion coupling (7, 10) and reduces insulin secretion in response to glucose, as well as reducing transcription of the insulin I gene (11). Expression of the transgene also leads to apoptosis in these cells after 48 h of induction (12).

During insulin biosynthesis, the nascent chain is translocated into the endoplasmic reticulum (ER), where it is folded into the correct conformation by the chaperone BiP (13), and the disulfide bonds are formed by protein-disulfide isomerase. Because insulin makes up to 14% of the total protein produced by the β-cell, it is clear that ER function must be maintained to allow sufficient insulin production to control blood glucose homeostasis. When the β-cell responds to high blood glucose by up-regulating insulin translation (14), the demand on the ER protein folding machinery can overwhelm its ability to process the incoming nascent proteins. The condition known as ER stress occurs when the protein folding and processing capacity of the ER is perturbed, either by increased protein load or by interference with the folding machinery (15, 16). The initial response to

* This work was supported by an European Foundation for the Study of Diabetes/Lilly grant, Swiss National Science Foundation Grant 310000-116750/1, and EuroDia 6th Framework Programme Grant LSHM-CT-2006-518153.

[S] The on-line version of this article (available at http://www.jbc.org) contains supplemental Tables S1–S3 and Figs. 1–5.

[1] To whom correspondence should be addressed. Tel.: 41-22-379-5548; Fax: 41-22-379-5260; E-mail: claes.wollheim@unige.ch.

[2] The abbreviations used are: MODY, maturity onset diabetes of the young; ActD, actinomycin D; CPA, cyclopiazonic acid; DN, dominant negative; Dox, doxycycline; ER, endoplasmic reticulum; MTT, 3-(4,5-dimethylthiazolyl-2)-2,5-diphenyl tetrazolium bromide; RIP, rat insulin 2 promoter; TUDCA, tauroursodeoxycholate; Q-PCR, quantitative PCR.

ER stress involves transcriptional induction of ER chaperones to normalize the unfolded protein load in the ER while simultaneously reducing translation to reduce the rate of unfolded protein entry into the ER (17). If these mechanisms fail to restore normal protein folding in the ER, apoptosis is induced through up-regulation of the transcription factor CHOP (18). Several *in vitro* studies have shown that inducing ER stress leads to cell death (19–22), and this has also been observed in mouse models of type 2 diabetes, including the db/db mouse (23) and the Akita mouse, which carries a point mutation in the insulin 2 gene (13). Importantly, in the Akita mouse, diabetes resulted purely as a consequence of insulin misfolding leading to ER stress in the absence of any defect of insulin production or sensitivity, showing that ER stress can play a causal role in diabetes development. Cell lines established from β-cells of these mice exhibited continuous activation of the master regulators of the ER stress response, ATF6 and XBP1 (24). Examination of postmortem sections of pancreata from normal compared with type 2 diabetic subjects showed up-regulation of ER stress markers, including BiP, DnaJC3 ($p58^{IPK}$), and CHOP in the pancreata from diabetic subjects (23). *Ex vivo*, islets from human type 2 diabetic donors are more sensitive to ER stress induced by high glucose than islets from control individuals (25). Therefore, ER stress can be considered as a factor in the development of multiple types of diabetes, whether induced by environmental or genetic factors.

In our laboratory, a transgenic mouse has been developed, which expresses the same DN *Hnf1α* gene as the DN *Hnf1α* cell line (7). Whereas the INS DN *Hnf1α* cell line has the transgene under the control of the Tet-On system, in the mice, the transgene was placed under the control of the rat insulin 2 promoter (RIP) so that expression would be restricted to the β-cells of the islet and (to a lesser extent) the brain (26). These mice developed diabetes at 6 weeks of age. Male mice exhibited defects in insulin secretion and loss of β-cell mass, recapitulating the MODY3 phenotype (27), in contrast to the *Hnf1α* global knockout mouse, which exhibits pleiotropic effects (28), and the heterozygous $Hnf1\alpha^{+/-}$ mouse, which does not develop diabetes (29). Ultrastructural analysis of islets of 6-week-old RIP-DN *Hnf1α* mice showed that the β-cells were highly disorganized with swollen mitochondria, dilated ER cisternae (a morphological sign of ER stress also observed in the Akita mouse), and fewer mature secretory granules. This led us to investigate whether HNF1α dysfunction was associated with β-cell ER stress. Here we used the INS DN *Hnf1α* cell line to demonstrate that HNF1α controls transcription of *Xbp1*, a master regulator of the ER stress response. We also demonstrate that XBP1 is required not only during ER stress but for maintenance of basal transcription of the major ER chaperone *BiP*, responsible for insulin folding in the ER. Analysis of islets from the RIP-DN *Hnf1α* transgenic mouse revealed attenuated *BiP* mRNA levels and increased sensitivity to cyclopiazonic acid (CPA)-induced apoptosis, suggesting that this mechanism is also operating *in vivo*. These data support a novel ER-related role for HNF1α in the β-cell.

## EXPERIMENTAL PROCEDURES

*Materials*—Cyclopiazonic acid (CPA), actinomycin D (ActD), tauroursodeoxycholate (TUDCA), Histopaque, and anti-rabbit IgG HRP conjugate were obtained from Sigma (Basel, Switzerland). Details of antibodies used for Western blotting are provided in supplemental Table S1. Cell culture media, transfection reagents and media, and fluorescent secondary antibodies were obtained from Invitrogen (Basel, Switzerland).

*Cell Culture*—INS DN *Hnf1α*, INS WT *Hnf1α*, and INS-1E cells were cultured as described previously (7, 30). Immunofluorescence of INS DN *Hnf1α* cells was performed as described (31).

*Quantitative RT-PCR*—RNA extraction, cDNA synthesis, and Q-PCR reactions were performed as described (31) except that genomic DNA was removed by DNase I digestion (Ambion/Applied Biosystems, Rotkreuz, Switzerland) prior to cDNA synthesis. Primer sequences are provided in supplemental Table S2. All transcripts were normalized to the housekeeping gene *Rps29* unless otherwise stated. Test reactions were performed on DNase I-treated RNA to ensure that no product was amplified from contaminating DNA.

*Cell Viability Assays*—The 3-(4,5-dimethylthiazolyl-2)-2,5-diphenyl tetrazolium bromide (MTT) assay was used to assess cell viability as described (32). Apoptosis was quantified with the Cell Death Detection $ELISA^{PLUS}$ kit (Roche Applied Science) according to the manufacturer's instructions, except that cells were seeded in 24-well plates at a density of $1.5 \times 10^5$ cells/well for the ELISA analysis.

*Cytosolic and Mitochondrial Calcium Measurements*—Cytosolic and mitochondrial calcium measurements were performed as described (33, 34). Cells were plated onto polyornithine-coated coverslips and infected with adenoviruses expressing either cytosolic or mitochondrially targeted aequorin under the control of the chicken actin promoter. After a 24-h induction of the transgene, DN *Hnf1α*-induced and uninduced cells were loaded with 5 μM coelenterazine (Calbiochem/Merck) for 2 h at 37 °C. The cells were perifused with KRBH buffer containing 2.5 mM glucose at a rate of 1 ml/min. Luminescence was measured using a photomultiplier apparatus (EMI 9789, Thorn EMI Electron Tubes Ltd.).

*Western Blotting*—Protein extraction and Western blotting were performed as described (32). Images were recorded using a LAS-4000 imager equipped with a CCD camera (Fujifilm, Dusseldorf, Germany). Densitometry was calculated by the Multigauge software (Fujifilm).

*ChIP and EMSA*—ChIP was performed as described (35). Purified DNA (input or ChIP) was used as the template for PCR with primers designed to amplify a product including the HNF1α binding site of the insulin or *Xbp1* promoters or an unrelated product from the *MyoD* promoter (supplemental Table S3). Quantification of ChIP sample/input ratios was by the $2^{-(\Delta\Delta Ct)}$ method. Nuclear extracts were prepared as described (36). Biotin-labeled 20-mer oligonucleotides (supplemental Table S3) were obtained from Eurogentec (Liège, Belgium) and hybridized to form the probe. EMSA binding reactions, electrophoresis, and detection were performed as described (35).

*Luciferase Assays*—A 948-bp segment of the *Xbp1* promoter containing the HNF1α binding site was amplified by PCR with primers xbp1_5′ and xbp1_3′ (supplemental Table S3) from

INS-1E total DNA and cloned into the vector pGEM-T Easy (Promega, Dübendorf, Switzerland). After sequencing, the amplicon was excised and cloned into the SmaI site of the pGL3 Basic luciferase reporter vector (Promega). The resulting construct (3 μg) was transfected into DN *Hnf1α* or WT *Hnf1α* cells with Lipofectamine 2000 along with the pSV-β-galactosidase vector (1 μg) (Promega) to normalize for transfection efficiency. Transfected cells were incubated with doxycycline (Dox) for the indicated times (in duplicate) prior to the assay for luciferase and β-galactosidase activity. Luciferase and β-galactosidase assays were performed as described (35), and the data were expressed as ratio of luciferase to β-galactosidase activity.

*Adenovirus Production and Infection*—Ad-LacZ (Clontech, Mountain View, CA), Ad-DN ATF6, and Ad-DN XBP1 (37) were amplified in HEK293 cells and purified by ultracentrifugation in a CsCl gradient followed by Sepharose column desalting. Adenoviral infection was for 2 h at 37 °C, and then the cells were washed and replenished with fresh medium, and incubation continued for the indicated times.

*Mouse Islet Isolation and Analysis*—The founder mice (26) had been backcrossed for 10 generations to achieve genetic homogeneity (27). Full details of genotypes and breeding were described previously (26, 27). Animals were housed and treated in accordance with institutional ethical guidelines. All experiments were performed on male mice at the age of 12–15 weeks. Glycemia was measured using a glucose electrode on blood samples from the tail vein. Islets were isolated by collagenase digestion followed by purification on a Histopaque gradient and hand picking and cultured prior to experiments in RPMI 1640 medium (Invitrogen). RNA was extracted using the Qiagen RNEasy Micro kit, including a DNase I digestion step, followed by reverse transcription as described for INS cells. For immunofluorescence (including TUNEL), islets were dissociated with trypsin immediately after isolation, and the cells were fixed to microscope slides by Cytospin. Thereafter, the immunofluorescence protocol was identical to that performed on INS cells. The TUNEL assay was performed according to the manufacturer's instructions (Roche Applied Science). For islet insulin measurements, batches of 20 islets (2–5 replicates/mouse) were extracted overnight with 10% acetic acid in ethanol and insulin measured by a rat insulin enzyme-linked immunoassay (SPI Bio, Montigny le Bretonneux, France). For analysis of apoptosis with and without CPA, islets were seeded in adherent 96-well plates at a density of 50 islets/well, and apoptosis was measured with the Cell Death Detection ELISA$^{PLUS}$ kit (Roche Applied Science).

*Bioinformatics*—Promoter sequences were extracted from the NCBI nucleotide data base and compared against the TransFac library of binding site matrices using the program Match (available from the "Gene Regulation" Web site) set to minimize false positives unless otherwise stated.

*Statistical Analysis*—Pairwise comparisons were performed by unpaired Student's *t* test unless otherwise stated, and multiple comparisons by one-way analysis of variance followed by Fisher's LSD post-hoc test (Figs. 6 and 7). $p < 0.05$ was considered significant. Pooled data are represented as mean ± S.E. unless otherwise stated. For all analyses, significance is indicated as follows: *, $p < 0.05$; **, $p < 0.01$; ***, $p < 0.001$.

## RESULTS

*Overexpression of DN Hnf1α Induces an Atypical ER Stress Response*—We focused this study on DN HNF1α (Fig. 1*A*) because endogenous HNF1α expression in β-cells is extremely low relative to other tissues (38), making it an unsuitable target for siRNA-mediated knockdown due to the difficulty of confirming whether gene expression has been efficiently suppressed. DN HNF1α protein in INS DN *Hnf1α* cells was strongly overexpressed after treatment with Dox (Fig. 1*B*), present in >95% of cells and localized to the nucleus with no sign of accumulation in the ER (Fig. 1*C*). Transcription of ER stress-associated genes was measured in INS DN *Hnf1α* cells with or without 48 h of Dox treatment. *Atf4* was increased after DN *Hnf1α* induction, but *BiP*, *CHOP*, and protein-disulfide isomerase were unchanged, whereas *Xbp1* was down-regulated (Fig. 1*D*). This contrasted with the classical ER stress response, where transcription of all of these genes would be expected to increase in conditions of ER stress (39). INS cells overexpressing DN *Hnf4α* (the MODY1 gene), were also tested for ER stress gene transcription, and no Dox-dependent changes were seen in these cells (Fig. 1*E*) or in INS-1E cells carrying no transgene (not shown). The effect of DN HNF1α overexpression appeared to be cumulative because we observed a progressive decrease of *Xbp1* transcript over time (supplemental Fig. 1*A*) despite the protein level of DN HNF1α being constant between 24 and 48 h of induction. Therefore, HNF1α dysfunction causes an atypical response that differs from the general induction of chaperones normally observed during ER stress.

*DN Hnf1α Attenuates the Transcriptional Response to ER Stress and Sensitizes Cells to ER Stress-induced Apoptosis*—CPA causes ER stress by preventing calcium uptake through the sarco/endoplasmic reticulum calcium ATPase pumps into the ER, depleting it of calcium and preventing the correct functioning of ER chaperones. Pilot experiments showed that inducing "physiological" ER stress with high glucose (16) for up to 48 h did not affect transcription of *BiP*, *Chop*, or *Atf4* with or without Dox in this cell line (not shown), so this was not studied further. Transcription of ER stress genes increased upon exposure to CPA. However, for *BiP*, this increase was attenuated when DN HNF1α was expressed (Fig. 2*A*), whereas *Chop* was unaffected (Fig. 2*B*). Protein-disulfide isomerase and *DnaJC3* mRNAs were affected similarly to *BiP* (Fig. 2, *C* and *D*). Other transcripts, including *Atf4* and *Xbp1* (supplemental Fig. 1, *B* and *C*), were unaffected by DN *Hnf1α* induction prior to CPA addition, suggesting that there are HNF1α-dependent and -independent modes of regulation of different ER stress genes. The effect of DN *Hnf1α* on CPA-induced cell death was assessed using the MTT assay and by measurement of release of cytoplasmic nucleosomes. Significantly more cell death was observed at 20 and 40 μM CPA in cells expressing DN *Hnf1α* (Fig. 2, *E* and *F*). Therefore, DN *Hnf1α* expression sensitizes cells to ER stress-induced apoptosis, probably by preventing normal transcriptional induction of chaperone genes.

*DN Hnf1α Alters Calcium Homeostasis*—In addition to its role in protein folding, the ER is crucial for the regulation of calcium homeostasis (40, 41). Given the link between DN *Hnf1α* and the ER stress response, we studied calcium signaling

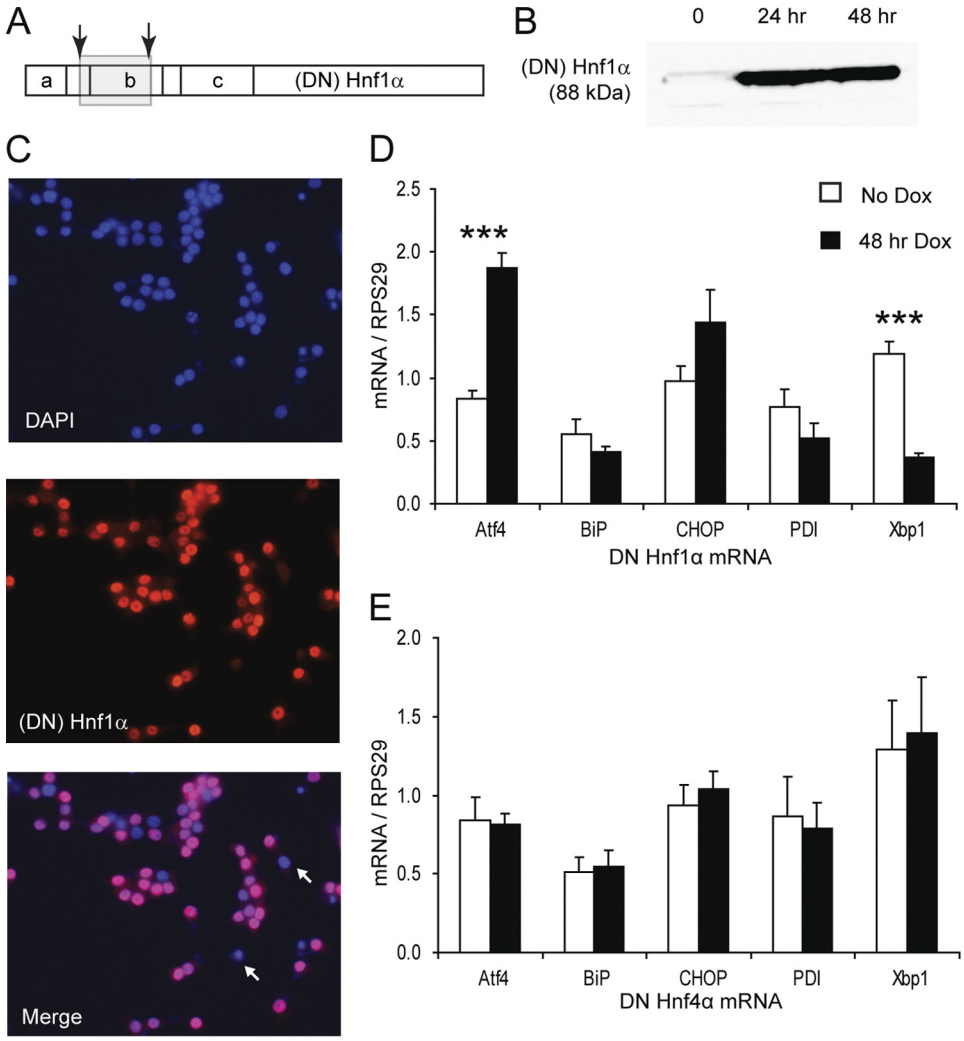


FIGURE 1. **DN HNF1α provokes an atypical ER stress response.** *A*, map of HNF1α domain structure with positions of DN HNF1α frameshift mutations indicated by *arrows*. *a*, dimerization domain; *b*, DNA binding (POU-like) domain; *c*, homeodomain-like region. The *gray box* indicates the region mistranslated in the DN mutant due to the frameshifts. *B*, Western blot for HNF1α (4 μg of nuclear extracts/lane) after 0, 24, or 48 h of 500 ng/ml Dox. *C*, immunofluorescence for (DN) HNF1α after 48 h of Dox. Two non-expressing cells are marked with *arrows*. *D*, Q-PCR of ER stress genes with or without 48 h of Dox in INS DN *Hnf1α* cells ($n = 4$). *E*, Q-PCR of ER stress genes with or without 48 h of Dox in INS DN *Hnf4α* cells ($n = 4$). *Error bars*, S.E.

after induction of the transgene for 24 h. Cytoplasmic calcium rises were induced by carbachol, CPA, or KCl and in all cases were higher in cells overexpressing DN *Hnf1α* (Fig. 3, *A–C*). However, using the same stimuli, mitochondrial calcium rises were unchanged following trangene induction (Fig. 3, *D–F*). Therefore, the enhanced cytoplasmic calcium responses are not due to inefficient calcium sequestering by mitochondria. Because cytoplasmic calcium responses were increased following the addition of CPA (which blocks uptake into the ER) as well as carbachol (which induces opening of ER calcium channels), we conclude that increased calcium mobilization from the ER does not explain the enhanced cytosolic calcium rises. We observed that the basal calcium concentration was elevated in DN *Hnf1α* cells (Fig. 3*G*) but that it was lowered to the same level in induced and uninduced cells after removal of extracellular calcium. This suggests that calcium influx from the extracellular space is increased in DN *Hnf1α* cells, perhaps due to enhanced store-operated calcium entry. This was tested by depleting the ER of calcium following the removal of calcium from the medium and stimulation with CPA. Readdition of extracellular calcium indeed demonstrated enhanced store-operated calcium entry in DN *Hnf1α* cells (Fig. 3*H*). Therefore, calcium handling by the ER and cytoplasm is already imbalanced after 24 h of DN *Hnf1α* expression, whereas mitochondrial calcium handling remains unchanged.

*DN Hnf1α Prevents Activation of XBP1 at the Protein Level in Response to ER Stress*—Upon ER stress, XBP1 is activated by mRNA splicing, where a 26-nucleotide intron is excised by the ER stress sensor Ire1, leading to a reading frameshift and production of a larger isoform of the protein, which is capable of transcribing its target genes (42). We quantified protein levels of BiP and the two isoforms of XBP1 (Fig. 4, *A–D*). Dox did not alter BiP or 54 kDa (active) XBP1, but it decreased 29 kDa (inactive) XBP1, consistent with the Dox-induced decrease in *Xbp1* mRNA. CPA alone did not affect 29 kDa XBP1, probably because transcription of the *Xbp1* precursor RNA is increased by CPA under these conditions (supplemental Fig. 1*C*). CPA increased BiP and 54 kDa XBP1, and this increase was attenuated for both proteins in the presence of CPA plus Dox. CPA plus Dox decreased 29 kDa XBP1 to a greater extent than Dox

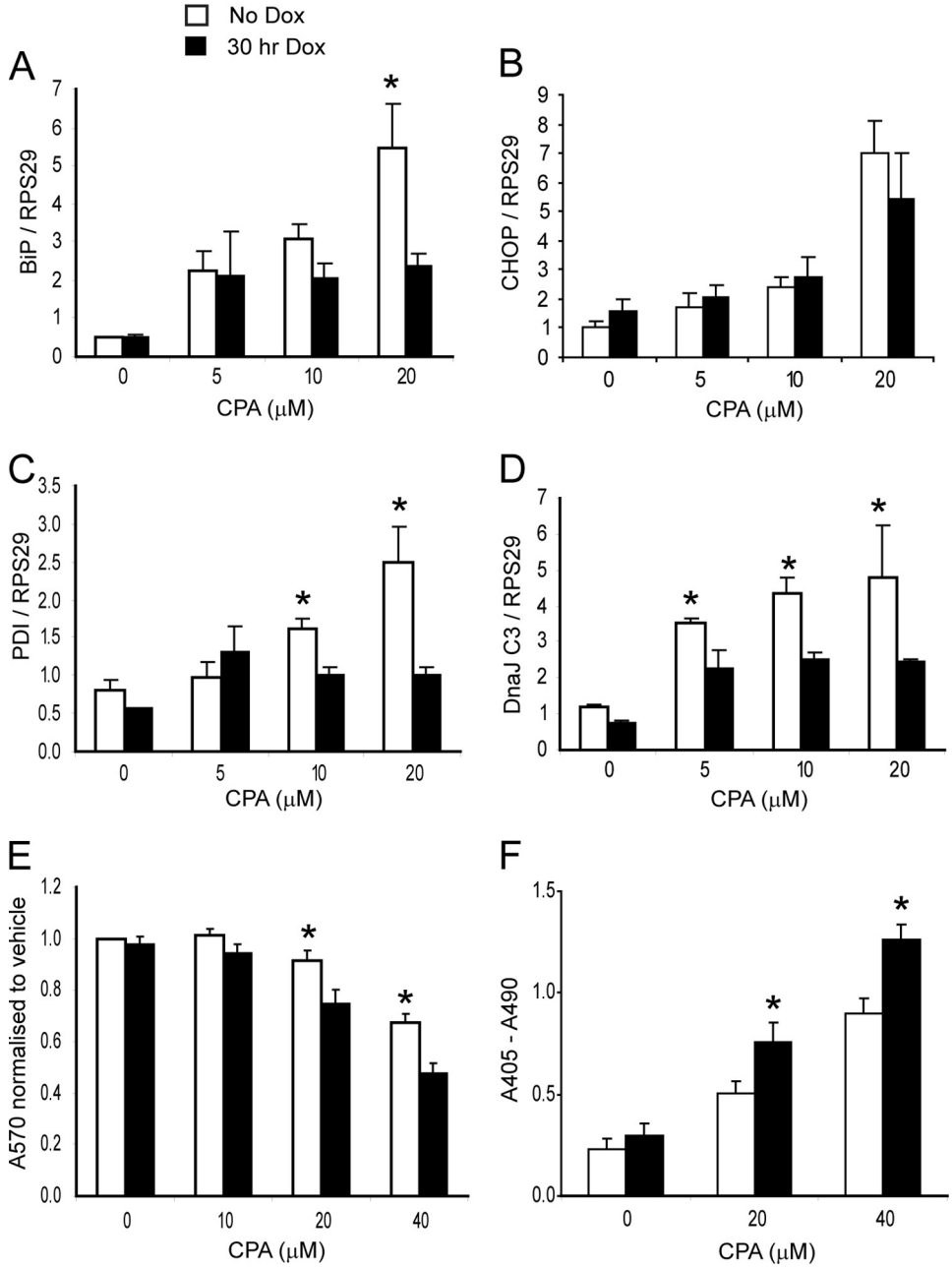


FIGURE 2. **ER stress-induced gene transcription is attenuated and cell death increased after induction of DN *Hnf1α*.** *A–D*, Q-PCR of BiP, CHOP, protein-disulfide isomerase (*PDI*), and DnaJ C3 mRNA after a dose response of CPA with or without 24-h preinduction of DN *Hnf1α* ($n = 3$). *E*, MTT assay of similarly treated cells ($n = 5$). Absorbance (570 nm) of the samples was normalized to that of the control. *F*, cell death ELISA$^{PLUS}$ apoptosis assay of similarly treated cells ($n = 4$). Data are shown as absolute absorbance values. *Error bars*, S.E.

alone. We conclude that activation of XBP1 in response to ER stress is reduced by DN *Hnf1α* induction, with consequences for the up-regulation of BiP, and that this is due to loss of the mRNA precursor, which is spliced by Ire1 to provide the mRNA of the active isoform. Under the same conditions, the active isoform of ATF6 showed no differences between conditions (Fig. 4*E*), and levels of the loading control GAPDH were consistently unchanged (Fig. 4*A*). Therefore, the attenuation of BiP protein production by DN *Hnf1α* is most likely mediated by loss of XBP1 rather than loss of ATF6.

*HNF1α Binds Directly to the Promoter of the Xbp1 Gene*—Promoter analysis of ER stress genes in the rat for HNF1α binding sites revealed one site, at 673 bases upstream of the transcription start site of *Xbp1*. A similar site was observed in the human *XBP1* gene at 569 bases upstream of the transcription start site and five sites (although with lower similarity to the consensus) in the mouse *Xbp1* gene (Fig. 5*A*). We analyzed binding of HNF1α to the *Xbp1* promoter *in vivo* by chromatin immunoprecipitation in a cell line overexpressing WT HNF1α (due to the low abundance of endogenous HNF1α). Specific products were amplified from the *Xbp1* and insulin promoters (Fig. 5*B*), whereas quantifiable chromatin precipitation was not observed for *Xbp1* with the negative control antibody (anti-ATF4) or for HNF1α with the negative control promoter

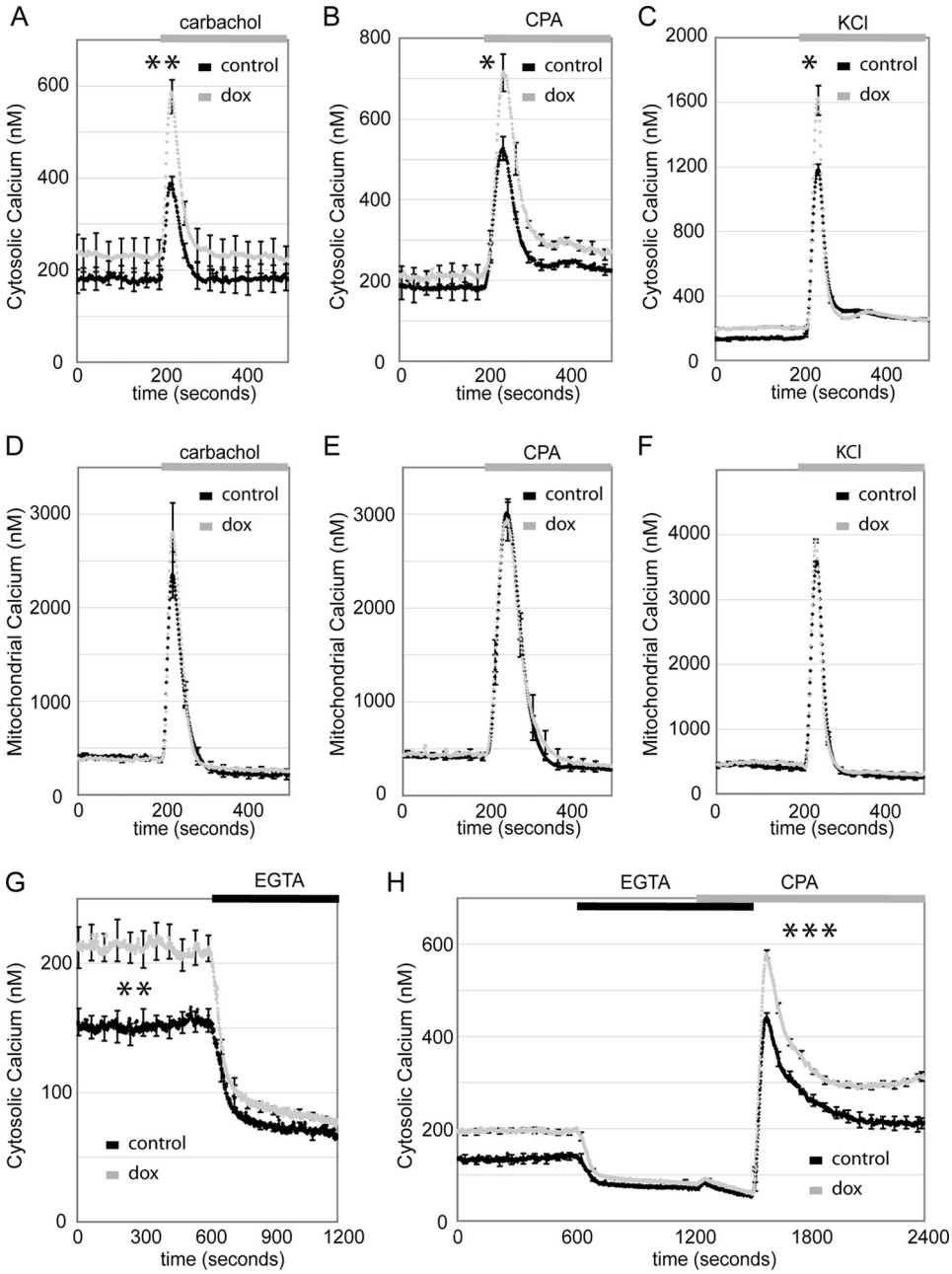


FIGURE 3. **DN HNF1α increases basal and stimulus-induced cytoplasmic calcium.** *A–C*, DN *Hnf1α* cells expressing cytosolic aequorin with or without 24 h of 500 ng/ml Dox. *A*, calcium mobilization from the ER induced by the muscarinic agonist carbachol (100 μM) ($n = 4$). *B*, ER calcium uptake blocked by CPA (20 μM) ($n = 3$). *C*, plasma membrane depolarized by KCl (30 mM) ($n = 3$). *D–F*, DN *Hnf1α* expressing mitochondrially targeted aequorin with or without 24 h of 500 ng/ml Dox. Carbachol, CPA, or KCl was added as indicated ($n = 3$ for each experiment). *G*, DN *Hnf1α* expressing cytosolic aequorin with or without 24 h of 500 ng/ml Dox, basal calcium before and after removal of extracellular calcium by supplementation of EGTA (0.4 mM) ($n = 7$). *H*, DN *Hnf1α* expressing cytosolic aequorin with or without 24 h of 500 ng/ml Dox. Removal of extracellular calcium was as in *G*. Readdition of calcium following CPA was as indicated to monitor store-operated calcium influx ($n = 4$).

(*MyoD*) (Fig. 5*C*). To examine the effect of DN *Hnf1α* on the *Xbp1* promoter, we prepared nuclear extracts from DN *Hnf1α* cells with or without Dox (48 h) and performed EMSAs with a probe corresponding to the HNF1α binding site (Fig. 5*D*). A band corresponding to HNF1α binding to the probe was observed in the untreated nuclear extract, which was eliminated by DN *Hnf1α* expression (*lane 3*), by the addition of anti-HNF1α to the binding reaction (*lanes 2* and *4*), or by increasing concentrations of the unlabeled probe (supplemental Fig. 2*A*). In summary, HNF1α binds to the *Xbp1* promoter, and binding is blocked by DN HNF1α (consistent with studies showing that this protein acts by preventing endogenous HNF1α from binding to DNA (9)).

The rat *Xbp1* promoter (supplemental Fig. 3) was cloned into a luciferase reporter plasmid and transfected into DN *Hnf1α* cells to analyze promoter activity. Although no difference was observed at 24 h of Dox, 48 h of Dox reduced the promoter activity (Fig. 5*E*), consistent with the EMSA results. When promoter activity was analyzed in WT *Hnf1α* cells, little effect was observed. Low doses of Dox for 24 h induced a slight but insig-

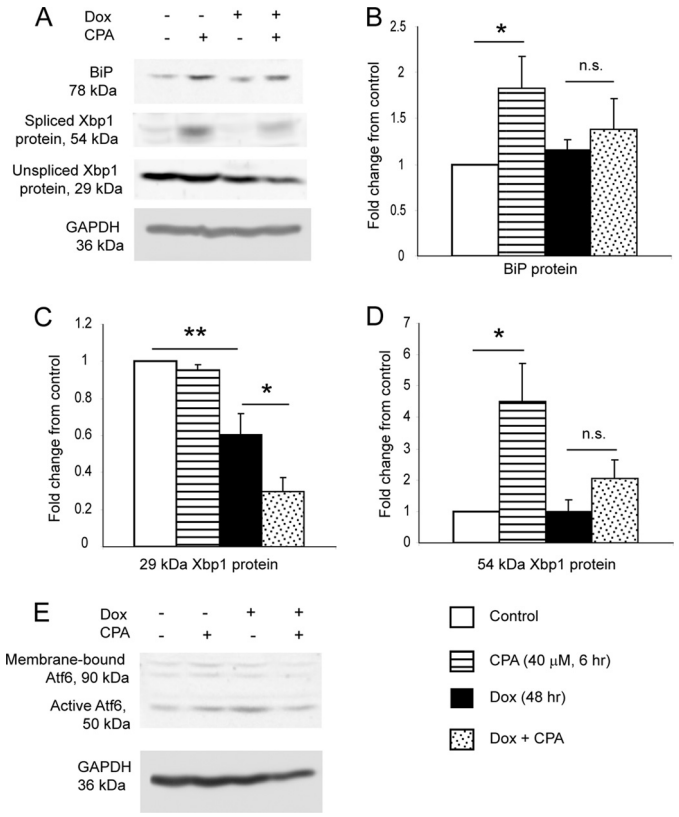


FIGURE 4. **Induction of DN HNF1α prevents CPA-induced increase in BiP and 54 kDa XBP1 protein and reduces 29 kDa XBP1 protein.** *A*, representative images of Western blots for BiP, both isoforms of XBP1, and GAPDH, after treatment with or without 48 h of Dox and 6 h of 40 μM CPA or vehicle (DMSO). *B*, densitometry quantification of BiP from Western blotting ($n = 4$). *C*, densitometry quantification of 29 kDa XBP1 from Western blotting ($n = 4$). *D*, densitometry quantification of 54 kDa XBP1 from Western blotting ($n = 4$). *E*, Western blot for ATF6 and GAPDH (representative image of two independent experiments). It is likely that the membrane-bound form of ATF6 is underrepresented in the image due to less efficient transfer of larger proteins to the membrane and/or less efficient extraction of membrane-bound proteins during cell lysate preparation. Numerical data are displayed as mean ± S.E. (*error bars*) of the -fold changes in intensity normalized to the untreated control sample. The increases (for BiP and 54 kDa XBP1) or decreases (for 29 kDa XBP1) in protein levels with CPA relative to vehicle were measured by unpaired one-tailed *t* test.

nificant increase in promoter activity (Fig. 5*F*), whereas pilot experiments with longer exposure times (48 h) or higher doses of Dox had no effect (not shown). Therefore, DN HNF1α reduces the activity of the promoter in INS cells, but overexpression of WT HNF1α is not sufficient to increase it. These data support a model where HNF1α binding to its site in the *Xbp1* promoter is required for basal transcription of *Xbp1*, but it is an essential accessory factor rather than a positive regulator capable of independently up-regulating *Xbp1*. Such a model has also been proposed for HNF1α target genes in embryonic liver (43). Given the importance of basal *Xbp1* expression, we then used ActD to examine the degradation rate of *Xbp1* and *BiP* mRNAs. *BiP* mRNA was unaffected either by 24-h Dox or 1-h ActD exposure (Fig. 5*G*). However, *Xbp1* mRNA was strongly decreased by 1 h of ActD with or without Dox (Fig. 5*H*). A time course of ActD confirmed that the rate of degradation was similar for both mRNAs with or without Dox (supplemental Fig. 2*B*). We conclude that *Xbp1* mRNA is unstable and that maintenance of basal levels of *Xbp1* transcript depends on *de novo* transcription for which HNF1α binding is required.

*Loss of XBP1 Function Is Toxic and Reduces Transcription of Endogenous XBP1 and BiP*—HNF1α is a regulator of multiple genes involved in β-cell development and function. Its dysfunction results in pleiotropic effects on metabolism-secretion coupling, which may impact on the ER in these cells. In order to examine the effects of loss of XBP1 in INS-1E cells with normal HNF1α function, we employed adenovirus vectors overexpressing DN forms of XBP1 or ATF6 (37) compared with a control adenovirus (Ad-LacZ). Surprisingly, we found that Ad-DN ATF6 and Ad-DN XBP1 were toxic to the cells even in the absence of an ER stress stimulus (Fig. 6*A*). Ad-LacZ was not toxic to the cells even at the highest dose tested (160 virus units/cell). However, both Ad-DN XBP1 and Ad-DN ATF6 caused significant cell death, which reached a maximum at 80 virus units/cell, and Ad-DN XBP1 appeared to be more toxic than Ad-DN ATF6. Immunofluorescence showed that 20 virus units/cell resulted in infection rates of ~90–95% (supplemental Fig. 4*A*), and DN ATF6 protein levels were comparable with endogenous ATF6 (supplemental Fig. 4*B*), so ER stress gene expression was examined at this virus titer. *BiP* expression was suppressed by both Ad-DN ATF6 and Ad-DN XBP1 with or without CPA (Fig. 6*B*), whereas *Atf4* was only affected by Ad-DN *Atf6* plus CPA (Fig. 6*C*), and *Chop* was unaffected (Fig. 6*D*). Endogenous *Atf6* was reduced with CPA by Ad-DN *Atf6* and Ad-DN *Xbp1* (but not at the basal level; Fig. 6*E*), whereas endogenous *Xbp1* was suppressed by both similarly to *BiP* (Fig. 6*F*). Therefore, although ATF6 and XBP1 are both required for ER stress-induced transcription of these genes, as previously reported (44), it appears that they are also required for basal transcription of *BiP* and *Xbp1* in the β-cell. Furthermore, in the presence of DN XBP1, ATF6 cannot compensate for XBP1 loss of function in the presence or absence of ER stress.

*Increased Sensitivity to CPA in DN Hnf1α-expressing Cells Is Partially Rescued by TUDCA*—If the sensitization to ER stress observed in DN *Hnf1α* cells is due to loss of XBP1-mediated chaperone production, then boosting the protein folding capacity of DN *Hnf1α* cells should rescue this effect. However, we were reluctant to overexpress the active form of XBP1 protein because this has been shown to down-regulate insulin secretion, decrease levels of the β-cell factors Pdx1 and MafA, and cause apoptosis (45). Chemical chaperones such as TUDCA should not interfere with β-cell function in this manner, and they have been shown to protect against ER stress *in vivo* (46). We therefore carried out apoptosis measurements with 48 h TUDCA exposure. At 48 h of Dox, TUDCA had no effect (not shown). We therefore shortened the Dox exposure time to 30 h, when sensitization to CPA but unchanged basal cell death is observed (Fig. 2, *E* and *F*). With 30 h of Dox (Fig. 7), there was no protection from basal or high glucose-induced cell death in the presence of Dox, but the cells were partially protected against the increased CPA-induced cell death. Therefore, chemical chaperones can help compensate for the defective ER stress response in DN *Hnf1α*-induced cells, although this effect is only seen before Dox-induced cell death occurs.

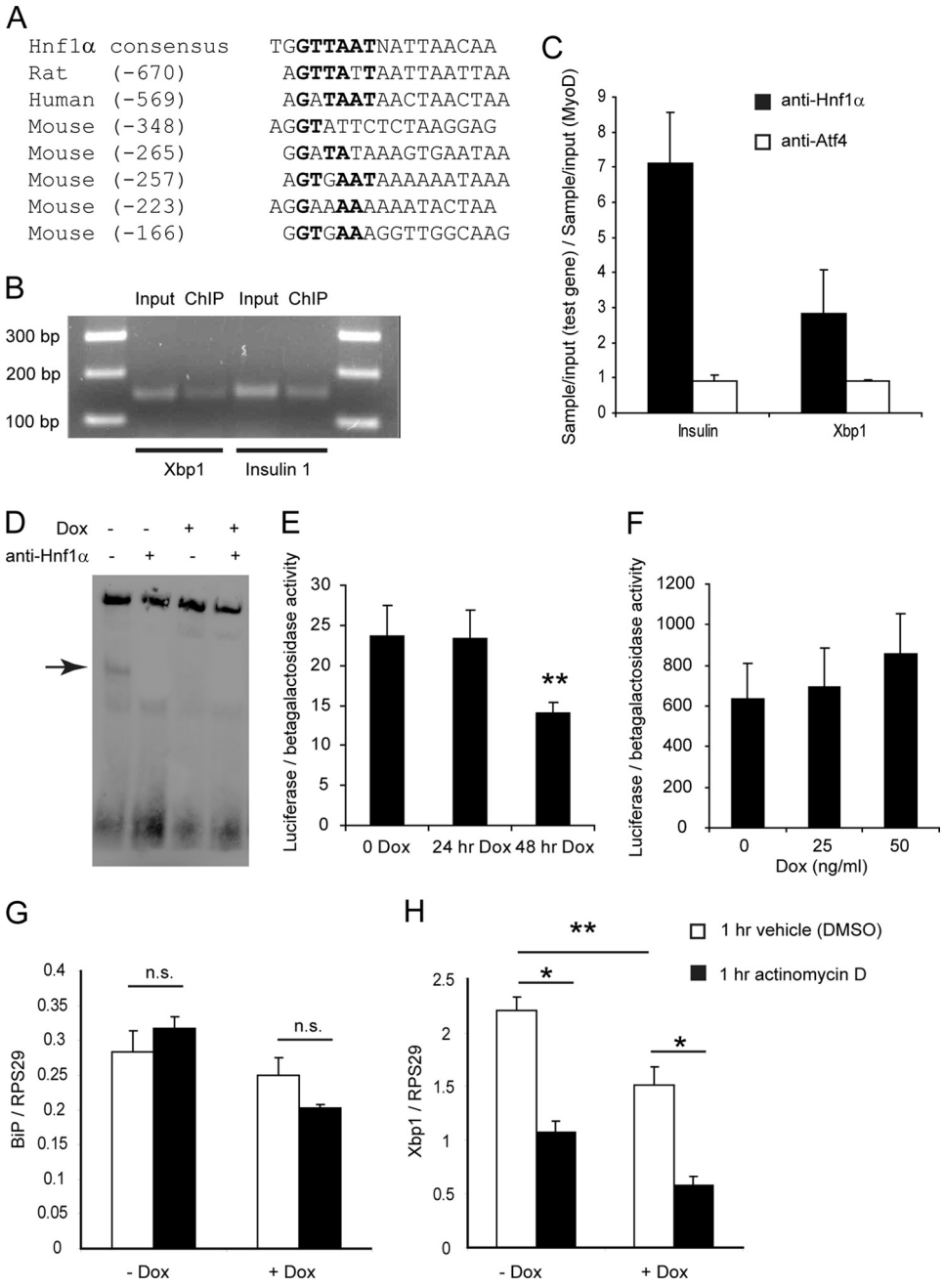


FIGURE 5. **HNF1α binds to the promoter of *Xbp1* and is required for basal *Xbp1* transcription.** *A*, alignment of sequences of HNF1α binding sites with the consensus sequence. The *numbers* in *parentheses* indicate the position of the site relative to the transcription start site of *Xbp1*. *B*, PCR products from ChIP with anti-HNF1α antibody and *Xbp1*-specific or insulin 1-specific primers (representative image of three experiments). *C*, quantitative PCR measurement of *Xbp1* and insulin promoter binding relative to negative control promoter and antibody. Values are the mean ± S.D. (*error bars*) of two independent experiments (separate from those of Fig. 5*B*), each analyzed in duplicate. *D*, EMSA to demonstrate binding of an oligonucleotide containing the HNF1α binding site in the rat *Xbp1* promoter to HNF1α *in vitro* (representative image of three experiments). The band corresponding to unique binding of HNF1α to the probe is marked with an *arrow*. *E*, luciferase assay of DN *Hnf1α* cells co-transfected with the *Xbp1* promoter-luciferase and the β-galactosidase reporter plasmids ($n = 4$). *F*, luciferase assay of WT *Hnf1α* cells co-transfected with the *Xbp1* promoter-luciferase and the β-galactosidase reporter plasmids ($n = 4$). *G* and *H*, *BiP* and *Xbp1* mRNA after 24 h with or without Dox, followed by 1 h with ActD or vehicle (DMSO) ($n = 3$).

*Islets of RIP-DN HNF1α Transgenic Mice Have Reduced Basal Levels of BiP and Are Sensitized to ER Stress-induced Apoptosis*—Fasting glycemia was measured to confirm that the transgenic mice were diabetic at the age when the experiments were performed (Fig. 8*A*), consistent with previous reports (26, 27). Upon measurement of ER stress gene transcription, RIP-DN *Hnf1α* islets had lower basal *BiP* and *Chop* mRNA relative to non-transgenic controls, although the response to CPA was intact (Fig. 8, *B* and *C*). Given the hyperglycemia observed in the transgenic animals, it was unexpected to find expression of these genes decreased, considering that high glucose *in vitro* is known to increase their expression in diabetic human islets (25). Although we had not observed an effect of glucose on ER stress gene expression in INS cells, 30 mM glucose induced an increase in *BiP* mRNA in control islets (79%; Fig. 8*D*), which was ablated in DN *Hnf1α* islets. *Chop* mRNA

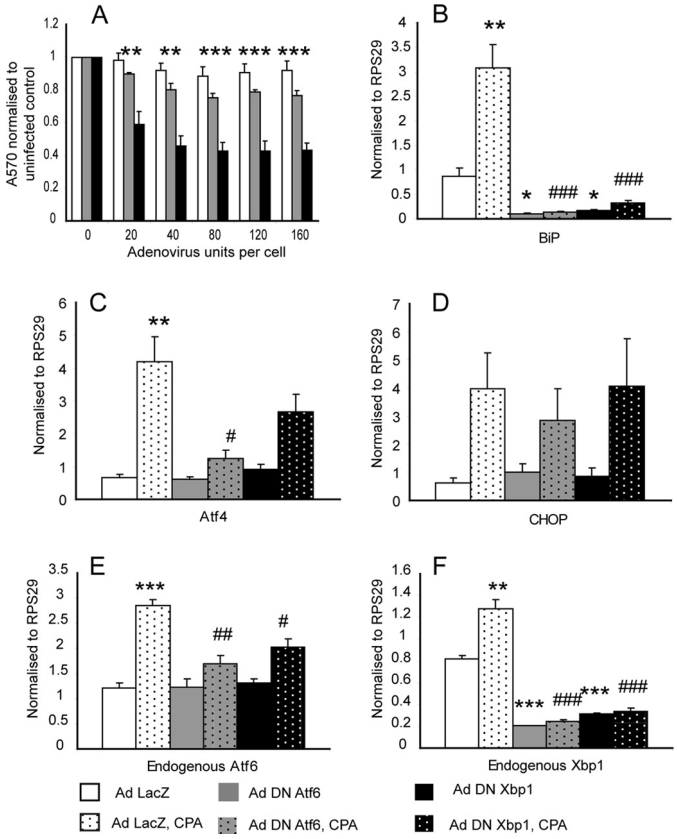


FIGURE 6. **DN XBP1 expression is toxic and has profound effects on ER stress gene transcription.** *A*, MTT assay of INS-1E cells after 24 h of infection with increasing doses of adenoviruses encoding LacZ, DN ATF6, and DN XBP1. ** and ***, $p < 0.01$ and $p < 0.001$, respectively, for pairwise comparison of DN ATF6 with DN XBP1 ($n = 3$). *B–F*, Q-PCR of *BiP*, *Atf4*, *Chop*, endogenous *Atf6*, and endogenous *Xbp1* mRNA in INS-1E cells after infection with 20 units/cell of the adenoviruses for 16 h followed by 20 μM CPA or vehicle for 6 h ($n = 3$). *, **, and ***, $p < 0.05$, $p < 0.01$, and $p < 0.001$ relative to LacZ plus vehicle control. #, ##, and ###, $p < 0.05$, $p < 0.01$, and $p < 0.001$ relative to LacZ plus CPA. *Error bars*, S.E.

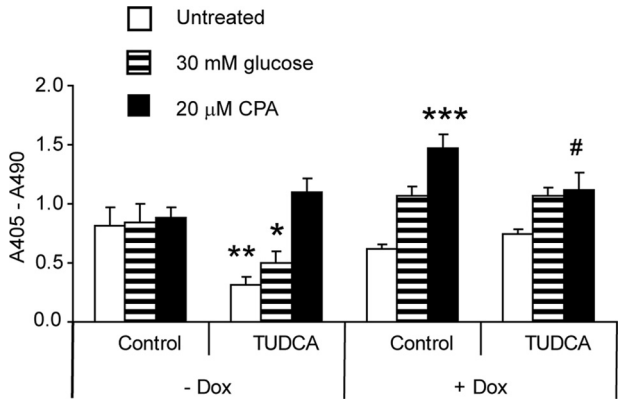


FIGURE 7. **The chemical chaperone TUDCA partially rescues DN *Hnf1α*-induced sensitivity to ER stress.** Apoptosis in DN *Hnf1α* cells with or without 48 h of 500 μg/ml TUDCA and 30 mM glucose, 30 h of 500 ng/ml Dox, and/or 6 h of 20 μM CPA or vehicle. *, **, and ***, $p < 0.05$, 0.01, and 0.001, respectively, relative to the control without Dox and without TUDCA. #, $p < 0.05$ relative to with Dox and without TUDCA. Data are displayed as mean ± S.E. (*error bars*) of four independent experiments.

expression was unaffected under these conditions (not shown). This suggests that the changes in expression of *BiP* and *Chop* in the transgenic islets are due to the transgene rather than hyperglycemia. Total *Xbp1* mRNA was measured in islets with or without CPA, and although there was a slight decrease of basal *Xbp1* in DN *Hnf1α* islets relative to the control, this was not significant (Fig. 8*E*). Similarly, spliced *Xbp1* was reduced in DN *Hnf1α* islets in the basal state, although the levels of this transcript were even more variable, and here also the difference was not significant (Fig. 8*F*). However, in these experiments, gene expression was measured in whole islets, whereas DN *Hnf1α* is only present in the β-cells. This would lead to an underestimation of the effects of HNF1α deficiency on spliced or total *Xbp1* mRNA using this model, because a reduced ER stress response in the DN *Hnf1α*-expressing β-cells would be masked by the intact ER stress response of the other islet cells. We therefore measured *Xbp1* in islets and liver from *Hnf1α* global knock-out mice. We observed a decrease in both tissues of the knock-out mice relative to controls (34% in islets, 35% in liver; Fig. 8*G*). These findings show that *Xbp1* expression is lowered in a separate model of HNF1α loss, independent of dominant negative dysfunction.

To estimate β-cell function, we measured islet insulin content and found that islets from the transgenic mice had insulin content reduced by 54% (Fig. 8*H*). Reduced islet insulin content is also seen in the Akita mouse, where extreme ER stress is the direct cause of diabetes (13). Apoptosis in freshly isolated islets was measured by the TUNEL assay with insulin immunostaining to identify apoptotic β-cells, showing a 3-fold increase in apoptotic β-cells in the DN *Hnf1α* islets relative to controls (Fig. 8*I*). Finally, we analyzed the apoptotic effect of CPA on the islets by cytoplasmic nucleosome release. CPA provoked a 10.2% increase in apoptosis in control islets relative to vehicle but a 31.8% increase in apoptosis in RIP-DN *Hnf1α* islets (Fig. 8*J*). We conclude that the islets of the RIP-DN *Hnf1α* mouse are sensitized to ER stress, similarly to the DN *Hnf1α*-overexpressing cell line.

## DISCUSSION

We find that upon induction of DN *Hnf1α* in INS DN *Hnf1α* cells, binding of HNF1α to the *Xbp1* promoter is reduced, basal transcription of *Xbp1* is down-regulated, and the cells are sensitized to ER stress. Reduction of basal transcription leads to a decrease in steady state *Xbp1* mRNA levels because we show here that the transcript is unstable and requires constant *de novo* transcription to compensate for its high turnover. When ER stress is induced in the presence of DN HNF1α, there is insufficient substrate for Ire1 to produce the mRNA of the active XBP1 isoform, and therefore genes that require XBP1 for their transcription in response to stress are not up-regulated. The attenuation of the ER stress response increases cell death following induction of ER stress in DN *Hnf1α*-expressing cells. Inactivation of XBP1 by a dominant negative mechanism in INS-1E cells confirms that functional XBP1 is required for β-cell viability both in the presence and absence of ER stress. Notably, DN XBP1 was toxic after 24 h of adenovirus infection (with no apparent sensitization to CPA, data not shown), whereas DN HNF1α induced sensitization to CPA at 24 h of induction but death at 48 h, as reported previously (12). We hypothesize that a lesser amount of functional XBP1 remains in the DN *Hnf1α*-expressing cells, probably due to *Xbp1* transcription driven by other factors, such as ATF6 through the

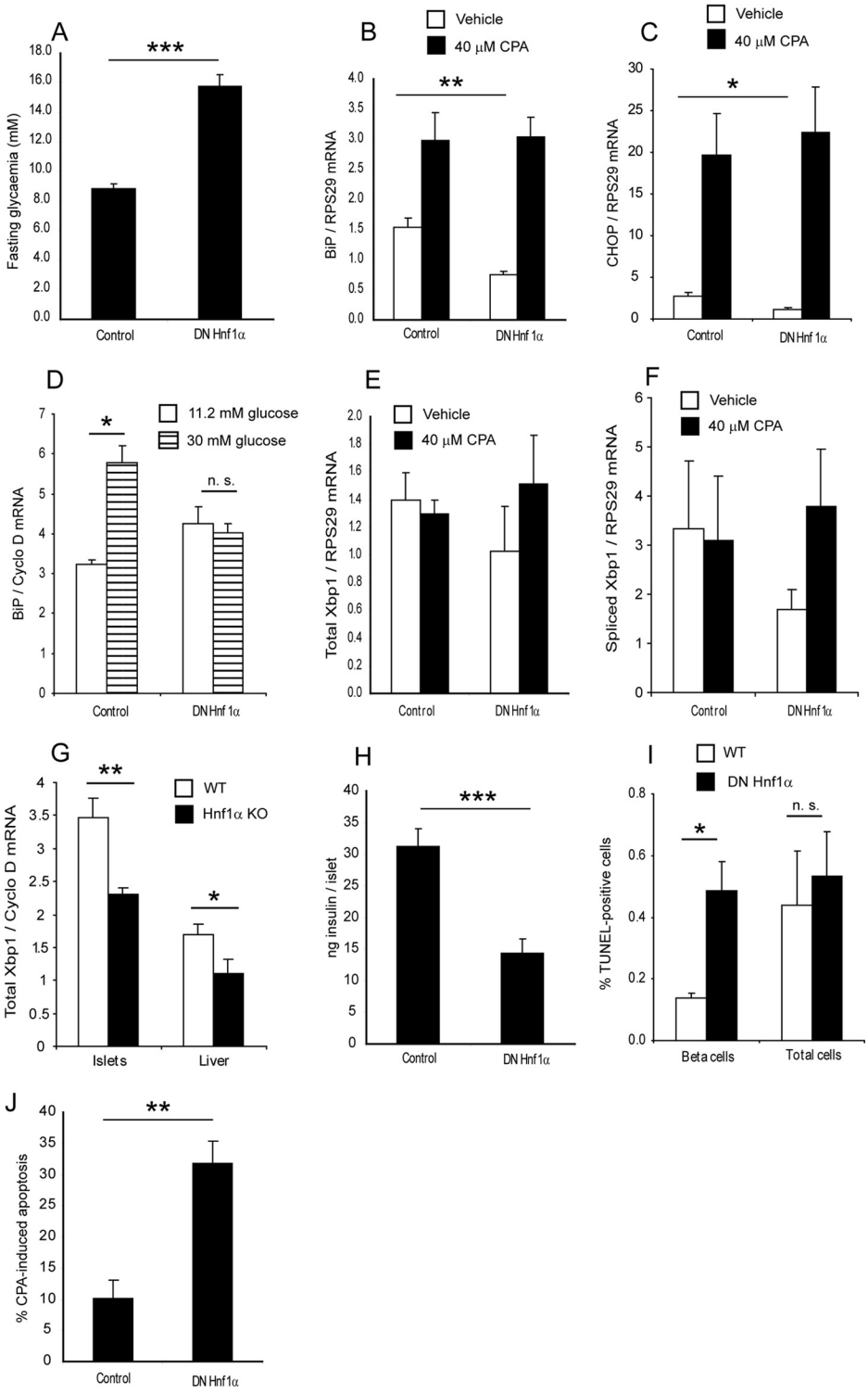


FIGURE 8. **RIP-DN *Hnf1α* mouse islets express less *BiP* and *Chop* mRNA and are sensitized to ER stress.** *A*, fasting glycemia of DN *Hnf1α* ($n = 19$) or littermate control ($n = 15$) mice. *B* and *C*, Q-PCR of *BiP* and *Chop* mRNA in control or DN *Hnf1α* islets after overnight culture followed by 6 h of 40 μM CPA or vehicle ($n = 3$). *D*, Q-PCR of *BiP* mRNA in control or DN *Hnf1α* islets with or without 30 mM glucose for 4 days ($n = 3$). Expression was normalized to cyclophilin D in this experiment because *Rps29* mRNA was increased by high glucose treatment (not shown). *E*, Q-PCR of total *Xbp1* mRNA in control or DN *Hnf1α* islets with or without 6 h of 40 μM CPA ($n = 3$). *F*, Q-PCR of spliced *Xbp1* mRNA in control or DN *Hnf1α* islets with or without 6 h of 40 μM CPA ($n = 3$). *G*, Q-PCR of total *Xbp1* mRNA in control or *Hnf1α* knock-out islets and liver ($n = 3$ wild type and 4 knock-out mice for islet expression and 6 wild type and 5 knock-out mice for liver expression). Four of the *Hnf1α* knock-out mice and two wild type mice were analyzed for both islet and liver expression; the remainder were different animals. Expression was normalized to cyclophilin D in this experiment because ribosomal protein mRNA expression can vary widely between tissues (58). *H*, islet insulin content of control or DN *Hnf1α* islets ($n = 6$ control and 6 DN *Hnf1α* mice). *I*, TUNEL assay for apoptosis in control or DN *Hnf1α* islets with insulin immunostaining to identify β-cells ($n = 3$ control and 4 DN *Hnf1α* mice). *J*, cell death ELISA$^{PLUS}$ assay of control or DN *Hnf1α* islets with or without 6 h of 40 μM CPA. Results are expressed as mean ± S.E. (*error bars*) of the percentage increase in cytoplasmic nucleosome content in the CPA-treated relative to the vehicle-treated islets ($n = 3$). For Q-PCR experiments with DN *Hnf1α* islets, islet mRNA was pooled from 2–5 mice each time. For Q-PCR with *Hnf1α* knock-out islets and liver, the islet insulin measurements and the apoptosis assay, samples from each mouse were analyzed individually.

NF-Y/ATF6 site in the *Xbp1* promoter (47) (supplemental Fig. 3) but insufficient for the normal functioning of the cell. This would explain the partial preservation of *Xbp1* promoter activity observed after 48 h of Dox in DN *Hnf1α*-expressing cells as well as the incomplete suppression of *Xbp1* mRNA in the *Hnf1α* knock-out mouse islets and liver. The combined data from the *Hnf1α* knock-out and DN *Hnf1α* cell and animal models support the hypothesis that HNF1α binding to the *Xbp1* promoter is essential for full *Xbp1* transcription and the β-cell ER stress response.

It has been reported that *BiP* is a transcriptional target of ATF6 during ER stress (44, 48) and that in MEFs, knock-out of *Atf6* has a larger effect on *BiP* transcription than knock-out of *Xbp1* (49). However, we show here that although ATF6 is indeed important for ER stress-induced *BiP* transcription, XBP1 is also required, and they are not redundant. Although DN ATF6 had equivalent or larger effects on ER stress gene transcription compared with DN XBP1, endogenous ATF6 was unable to compensate for lack of function of XBP1. It could have been possible that DN ATF6 and DN XBP1 both bind to the same *cis*-acting element in ER stress-responsive promoters and are therefore not exerting independent effects, but we do not believe this to be the case due to their differential effects on transcription of *Atf4* and on cell death. Interestingly, a recent study *in vivo* has shown that mice with *Xbp1* knocked out specifically in the β-cells had defective insulin processing, impaired glucose tolerance, and swollen ER and mitochondria (50), whereas mice lacking *Atf6* did not show any such defects (44, 51).

We also found that both ATF6 and XBP1 were required for basal transcription of BiP. It had previously been shown that basal transcription of BiP did not depend on the unfolded protein response pathway but on growth factor signaling (52). However, this study was performed on other cell lines, so this requirement of ATF6 and XBP1 for basal transcription of BiP may be unique to β-cells. It had been shown in INS cells that reduction of basal chaperone transcription by IFN-γ sensitizes cells to ER stress-induced cell death, in agreement with our findings, although the mechanism of basal transcription was not described (22). It has been suggested that *Atf6* and *Xbp1* are "housekeeping" rather than stress response genes in the β-cell (53), and our data are consistent with this hypothesis. It was recently reported that islets of *Pdx1* (MODY4) haploinsufficient mice are sensitized to ER stress through reduction of *Atf4* and its target genes (54), showing that another MODY gene can play an important role in maintenance of ER function as well as β-cell development. However, we observed a positive rather than negative effect of DN-*Hnf1α* on *Atf4* (Fig. 1*D*).

Altered calcium handling was already observed in the DN *Hnf1α* cells before the addition of calcium-raising stimuli, reflected in increased basal cytosolic calcium after only 24 h of Dox induction. ER calcium mobilization and plasma membrane depolarization caused higher calcium rises in the cytosol but not the mitochondria of DN *Hnf1α*-induced cells. When calcium stores were depleted in order to measure store-operated calcium entry (40), we observed increased activity in DN *Hnf1α*-expressing cells after 24 h of Dox. Although the DN *Hnf1α* cells and mice had lower mRNA levels of sarco/endoplasmic reticulum calcium ATPase 2b and/or 3 (*SERCA2b* and/or *SERCA3*) (supplemental Fig. 5), the higher peak of cytoplasmic calcium in the DN *Hnf1α*-expressing cells in response to CPA suggests that this does not explain the differences in calcium handling (CPA blocks ER calcium uptake completely whether or not DN *Hnf1α* is expressed). Rather, it seems that the ER defect is a result of DN *Hnf1α* induction affecting signaling to the plasma membrane to alter the equilibrium toward increased calcium influx. At this stage (24 h of DN *Hnf1α* induction), the mitochondrial calcium responses to the applied stimuli were similar between induced and non-induced DN *Hnf1α* cells. Therefore, the defective calcium homeostasis precedes mitochondrial dysfunction in these cells, suggesting that the observed mitochondrial defects are downstream of ER incapacitation caused by DN *Hnf1α*.

In previous studies of the RIP-DN HNF1α MODY3 mouse model (26), we found that these mice have a primary defect in β-cell function with impaired insulin secretion followed by loss of β-cell mass, similar to MODY3 patients. In the mice, the β-cells displayed dilated ER cisternae and fewer insulin secretory granules, suggesting a defect in ER function. Similar defects are seen in other types of secretory cells when XBP1 is blocked (55). Here we demonstrate that the ER defect is likely to arise from strong inhibition of XBP1 transcription by DN HNF1α, which impairs production of BiP. Failure to increase levels of this chaperone during ER stress would decrease the ability of the β-cell to tolerate metabolic stress and increase its sensitivity to apoptosis. It was notable that in the cell line, *BiP* mRNA production was not significantly impaired upon expression of the transgene alone, only in the presence of CPA, whereas in the RIP-DN *Hnf1α* mice, *BiP* was significantly reduced at the basal level, while the transcript level after CPA was the same as in the controls (it should be noted that islets from the RIP-DN *Hnf1α* mice only contain 50% β-cells, so 50% of the RNA comes from the other islet cell types). However, it was only possible to induce the DN *Hnf1α* transgene in the cell line for a maximum of 48 h, whereas the mice were analyzed at the age of 12–15 weeks (at which point they had been hyperglycemic for at least 6 weeks). Therefore, we consider the untreated islets in these mice to be physiologically more similar to the CPA-stressed state in the cell line.

The insulin-secreting cell lines used in this study have ~5–10% of the insulin content of a primary β-cell (7, 30), which would reduce the relative unfolded protein load in the ER in these cells. It is also possible that the suppression of XBP1 is naturally weaker in the DN *Hnf1α* islets than in the cell line because the RIP promoter does not induce DN *Hnf1α* as strongly as the Tet-On system used in the cell line. Alternatively, XBP1 regulation by HNF1α in the mouse may naturally differ from its regulation in the rat due to the different distribution of HNF1α binding sites in the *Xbp1* promoter (Fig. 5*A*). Nonetheless, the sensitivity of both the INS DN *Hnf1α* cells and the RIP-DN *Hnf1α* islets to ER stress-induced apoptosis suggests that the same mechanism is operating in both models. The lack of an increase in *Chop* expression suggests that the sensitivity to ER stress in the DN *Hnf1α* cells and islets leads to mitochondrially mediated cell death rather than inducing apoptosis through CHOP. It has been shown that ER stress can

induce mitochondrial apoptosis directly in response to acute ER stress stimulation in other cell types (56). A lack of increase in CHOP expression during an otherwise active ER stress response in β-cells was also observed by Kennedy *et al.* (57). The partial rescue of the DN *Hnf1α*-induced sensitivity to CPA by the chemical chaperone TUDCA shows that improving the protein folding capacity of the cells can (partially) compensate for the insufficient up-regulation of endogenous chaperones due to the lack of active XBP1. Together, these data suggest a new mechanism by which HNF1α dysfunction is toxic to β-cells and which may act upstream of the mitochondrial defects characterized previously (4, 7, 10). The contribution of HNF1α to ER function by maintenance of appropriate XBP1 levels is an intriguing new role for this transcription factor.

*Acknowledgments—We thank Dr. Maria Sörhede Winzell for helpful discussions regarding the DN Hnf1α mice. We acknowledge Dominique Duhamel, Dale Brighouse, and Deborah Aeberhard for general technical assistance and Dimitri Petrov and Xavi Garcia for expert assistance in purification of islets and RNA.*

## REFERENCES


1. Yamagata, K., Oda, N., Kaisaki, P. J., Menzel, S., Furuta, H., Vaxillaire, M., Southam, L., Cox, R. D., Lathrop, G. M., Boriraj, V. V., Chen, X., Cox, N. J., Oda, Y., Yano, H., Le Beau, M. M., Yamada, S., Nishigori, H., Takeda, J., Fajans, S. S., Hattersley, A. T., Iwasaki, N., Hansen, T., Pedersen, O., Polonsky, K. S., and Bell, G. I. (1996) *Nature* **384,** 455–458
2. Ryffel, G. U. (2001) *J. Mol. Endocrinol.* **27,** 11–29
3. Yamagata, K., Yang, Q., Yamamoto, K., Iwahashi, H., Miyagawa, J., Okita, K., Yoshiuchi, I., Miyazaki, J., Noguchi, T., Nakajima, H., Namba, M., Hanafusa, T., and Matsuzawa, Y. (1998) *Diabetes* **47,** 1231–1235
4. Wang, H., Antinozzi, P. A., Hagenfeldt, K. A., Maechler, P., and Wollheim, C. B. (2000) *EMBO J.* **19,** 4257–4264
5. Miquerol, L., Lopez, S., Cartier, N., Tulliez, M., Raymondjean, M., and Kahn, A. (1994) *J. Biol. Chem.* **269,** 8944–8951
6. Emens, L. A., Landers, D. W., and Moss, L. G. (1992) *Proc. Natl. Acad. Sci. U.S.A.* **89,** 7300–7304
7. Wang, H., Maechler, P., Hagenfeldt, K. A., and Wollheim, C. B. (1998) *EMBO J.* **17,** 6701–6713
8. Servitja, J. M., Pignatelli, M., Maestro, M. A., Cardalda, C., Boj, S. F., Lozano, J., Blanco, E., Lafuente, A., McCarthy, M. I., Sumoy, L., Guigó, R., and Ferrer, J. (2009) *Mol. Cell. Biol.* **29,** 2945–2959
9. Nicosia, A., Monaci, P., Tomei, L., De Francesco, R., Nuzzo, M., Stunnenberg, H., and Cortese, R. (1990) *Cell* **61,** 1225–1236
10. Pongratz, R. L., Kibbey, R. G., Kirkpatrick, C. L., Zhao, X., Pontoglio, M., Yaniv, M., Wollheim, C. B., Shulman, G. I., and Cline, G. W. (2009) *J. Biol. Chem.* **284,** 16808–16821
11. Okita, K., Yang, Q., Yamagata, K., Hangenfeldt, K. A., Miyagawa, J., Kajimoto, Y., Nakajima, H., Namba, M., Wollheim, C. B., Hanafusa, T., and Matsuzawa, Y. (1999) *Biochem. Biophys. Res. Commun.* **263,** 566–569
12. Wobser, H., Düssmann, H., Kögel, D., Wang, H., Reimertz, C., Wollheim, C. B., Byrne, M. M., and Prehn, J. H. (2002) *J. Biol. Chem.* **277,** 6413–6421
13. Wang, J., Takeuchi, T., Tanaka, S., Kubo, S. K., Kayo, T., Lu, D., Takata, K., Koizumi, A., and Izumi, T. (1999) *J. Clin. Invest.* **103,** 27–37
14. Wicksteed, B., Herbert, T. P., Alarcon, C., Lingohr, M. K., Moss, L. G., and Rhodes, C. J. (2001) *J. Biol. Chem.* **276,** 22553–22558
15. Scheuner, D., and Kaufman, R. J. (2008) *Endocr. Rev.* **29,** 317–333
16. Eizirik, D. L., Cardozo, A. K., and Cnop, M. (2008) *Endocr. Rev.* **29,** 42–61
17. Harding, H. P., Novoa, I., Zhang, Y., Zeng, H., Wek, R., Schapira, M., and Ron, D. (2000) *Mol. Cell* **6,** 1099–1108
18. Oyadomari, S., and Mori, M. (2004) *Cell Death Differ.* **11,** 381–389
19. Cardozo, A. K., Ortis, F., Storling, J., Feng, Y. M., Rasschaert, J., Tonnesen, M., Van Eylen, F., Mandrup-Poulsen, T., Herchuelz, A., and Eizirik, D. L. (2005) *Diabetes* **54,** 452–461
20. Kharroubi, I., Ladrière, L., Cardozo, A. K., Dogusan, Z., Cnop, M., and Eizirik, D. L. (2004) *Endocrinology* **145,** 5087–5096
21. Oyadomari, S., Takeda, K., Takiguchi, M., Gotoh, T., Matsumoto, M., Wada, I., Akira, S., Araki, E., and Mori, M. (2001) *Proc. Natl. Acad. Sci. U.S.A.* **98,** 10845–10850
22. Pirot, P., Eizirik, D. L., and Cardozo, A. K. (2006) *Diabetologia* **49,** 1229–1236
23. Laybutt, D. R., Preston, A. M., Akerfeldt, M. C., Kench, J. G., Busch, A. K., Biankin, A. V., and Biden, T. J. (2007) *Diabetologia* **50,** 752–763
24. Nozaki, J., Kubota, H., Yoshida, H., Naitoh, M., Goji, J., Yoshinaga, T., Mori, K., Koizumi, A., and Nagata, K. (2004) *Genes Cells* **9,** 261–270
25. Marchetti, P., Bugliani, M., Lupi, R., Marselli, L., Masini, M., Boggi, U., Filipponi, F., Weir, G. C., Eizirik, D. L., and Cnop, M. (2007) *Diabetologia* **50,** 2486–2494
26. Hagenfeldt-Johansson, K. A., Herrera, P. L., Wang, H., Gjinovci, A., Ishihara, H., and Wollheim, C. B. (2001) *Endocrinology* **142,** 5311–5320
27. Winzell, M. S., Pacini, G., Wollheim, C. B., and Ahren, B. (2004) *Diabetes* **53,** Suppl. 3, S92–S96
28. Pontoglio, M., Barra, J., Hadchouel, M., Doyen, A., Kress, C., Bach, J. P., Babinet, C., and Yaniv, M. (1996) *Cell* **84,** 575–585
29. Pontoglio, M., Sreenan, S., Roe, M., Pugh, W., Ostrega, D., Doyen, A., Pick, A. J., Baldwin, A., Velho, G., Froguel, P., Levisetti, M., Bonner-Weir, S., Bell, G. I., Yaniv, M., and Polonsky, K. S. (1998) *J. Clin. Invest.* **101,** 2215–2222
30. Merglen, A., Theander, S., Rubi, B., Chaffard, G., Wollheim, C. B., and Maechler, P. (2004) *Endocrinology* **145,** 667–678
31. Brun, T., Duhamel, D. L., Hu He, K. H., Wollheim, C. B., and Gauthier, B. R. (2007) *Oncogene* **26,** 4261–4271
32. Park, K. S., Wiederkehr, A., Kirkpatrick, C., Mattenberger, Y., Martinou, J. C., Marchetti, P., Demaurex, N., and Wollheim, C. B. (2008) *J. Biol. Chem.* **283,** 33347–33356
33. Ishihara, H., Maechler, P., Gjinovci, A., Herrera, P. L., and Wollheim, C. B. (2003) *Nat Cell Biol.* **5,** 330–335
34. Wiederkehr, A., Park, K. S., Dupont, O., Demaurex, N., Pozzan, T., Cline, G. W., and Wollheim, C. B. (2009) *EMBO J.* **28,** 417–428
35. Gauthier, B. R., Wiederkehr, A., Baquié, M., Dai, C., Powers, A. C., Kerr-Conte, J., Pattou, F., MacDonald, R. J., Ferrer, J., and Wollheim, C. B. (2009) *Cell Metab.* **10,** 110–118
36. Schreiber, E., Matthias, P., Müller, M. M., and Schaffner, W. (1988) *EMBO J.* **7,** 4221–4229
37. Yamaguchi, S., Ishihara, H., Yamada, T., Tamura, A., Usui, M., Tominaga, R., Munakata, Y., Satake, C., Katagiri, H., Tashiro, F., Aburatani, H., Tsukiyama-Kohara, K., Miyazaki, J., Sonenberg, N., and Oka, Y. (2008) *Cell Metab.* **7,** 269–276
38. Luco, R. F., Maestro, M. A., del Pozo, N., Philbrick, W. M., de la Ossa, P. P., and Ferrer, J. (2006) *Diabetes* **55,** 2202–2211
39. Elouil, H., Bensellam, M., Guiot, Y., Vander Mierde, D., Pascal, S. M., Schuit, F. C., and Jonas, J. C. (2007) *Diabetologia* **50,** 1442–1452
40. Rizzuto, R., and Pozzan, T. (2006) *Physiol. Rev.* **86,** 369–408
41. Maechler, P., Kennedy, E. D., Sebö, E., Valeva, A., Pozzan, T., and Wollheim, C. B. (1999) *J. Biol. Chem.* **274,** 12583–12592
42. Calfon, M., Zeng, H., Urano, F., Till, J. H., Hubbard, S. R., Harding, H. P., Clark, S. G., and Ron, D. (2002) *Nature* **415,** 92–96
43. Blumenfeld, M., Maury, M., Chouard, T., Yaniv, M., and Condamine, H. (1991) *Development* **113,** 589–599
44. Yamamoto, K., Sato, T., Matsui, T., Sato, M., Okada, T., Yoshida, H., Harada, A., and Mori, K. (2007) *Dev. Cell* **13,** 365–376
45. Allagnat, F., Christulia, F., Ortis, F., Pirot, P., Lortz, S., Lenzen, S., Eizirik, D. L., and Cardozo, A. K. (2010) *Diabetologia* **53,** 1120–1130
46. Ozcan, U., Yilmaz, E., Ozcan, L., Furuhashi, M., Vaillancourt, E., Smith, R. O., Görgün, C. Z., and Hotamisligil, G. S. (2006) *Science* **313,** 1137–1140
47. Yoshida, H., Matsui, T., Yamamoto, A., Okada, T., and Mori, K. (2001) *Cell* **107,** 881–891
48. Adachi, Y., Yamamoto, K., Okada, T., Yoshida, H., Harada, A., and Mori, K. (2008) *Cell Struct. Funct.* **33,** 75–89
49. Lee, A. H., Iwakoshi, N. N., and Glimcher, L. H. (2003) *Mol. Cell. Biol.* **23,** 7448–7459

50. Lee, A. H., Heidtman, K., Hotamisligil, G. S., and Glimcher, L. H. (2011) *Proc. Natl. Acad. Sci. U.S.A.* **108,** 8885–8890
51. Wu, J., Rutkowski, D. T., Dubois, M., Swathirajan, J., Saunders, T., Wang, J., Song, B., Yau, G. D., and Kaufman, R. J. (2007) *Dev. Cell* **13,** 351–364
52. Brewer, J. W., Cleveland, J. L., and Hendershot, L. M. (1997) *EMBO J.* **16,** 7207–7216
53. Kutlu, B., Burdick, D., Baxter, D., Rasschaert, J., Flamez, D., Eizirik, D. L., Welsh, N., Goodman, N., and Hood, L. (2009) *BMC Med. Genomics* **2,** 3
54. Sachdeva, M. M., Claiborn, K. C., Khoo, C., Yang, J., Groff, D. N., Mirmira, R. G., and Stoffers, D. A. (2009) *Proc. Natl. Acad. Sci. U.S.A.* **106,** 19090–19095
55. Lee, A. H., and Glimcher, L. H. (2009) *Cell Mol. Life Sci.* **66,** 2835–2850
56. Deniaud, A., Sharaf el dein, O., Maillier, E., Poncet, D., Kroemer, G., Lemaire, C., and Brenner, C. (2008) *Oncogene* **27,** 285–299
57. Kennedy, J., Katsuta, H., Jung, M. H., Marselli, L., Goldfine, A. B., Balis, U. J., Sgroi, D., Bonner-Weir, S., and Weir, G. C. (2010) *PLoS One* **5,** e11211
58. Thorrez, L., Van Deun, K., Tranchevent, L. C., Van Lommel, L., Engelen, K., Marchal, K., Moreau, Y., Van Mechelen, I., and Schuit, F. (2008) *PLoS One* **3,** e1854